Inorg. Chem. **2006**, *45*, 9864–9876

A Systematic Resolution of Sulfur in Reticulated Vitreous Carbon Using X-ray Absorption Spectroscopy

Patrick Frank,*[,†,‡] Serena DeBeer George,[‡] Elodie Anxolabéhère-Mallart,[†,§] Britt Hedman,[‡] and Keith O. Hodgson[†,‡]

Department of Chemistry, Stanford University, Stanford, California 94305, and Stanford Synchrotron Radiation Laboratory, SLAC, Stanford University, Stanford, California 94309

Received June 13, 2006

Sulfur K-edge X-ray absorption spectroscopy (XAS) was used to characterize the ∼0.1% sulfur found both in native reticulated vitreous carbon (RVC) foam and in RVC oxidatively modified using 0.2 M $KMnO_4$ in 2 M H_2SO_4. Sulfur valences and functional groups were assessed using K-edge XAS spectral curve-fitting and employing explicit sulfur compounds as models. For native RVC, these were episulfide (∼3%), thianthrene (∼9%), disulfide (∼10%), sulfenate ester (∼12%), benzothiophene (∼24%), *N*,*N*′-thiobisphthalimide (∼30%), alkyl sulfonate (∼1.2%), alkyl sulfate monoester (∼6%), and sulfate dianion (∼6%). Permanganate oxidation of RVC diminished sulfenic sulfur to ∼9%, thianthrenic sulfur to ∼7%, and sulfate dianion to ∼1% but increased sulfate monoester to ∼12%, and newly produced sulfone (∼2%) and sulfate diester (∼5%). A simple thermodynamic model was derived that allows proportionate functional group comparisons despite differing (∼ ±15%) total sulfur contents between RVC batches. The limits of accuracy in the XAS curve-fitting analysis are discussed in terms of microenvironments and extended structures in RVC carbon that cannot be exactly modeled by small molecules. Sulfate esters cover ∼0.15% of the RVC surface, increasing to ∼0.51% following permanganate/sulfuric acid treatment. The detection of episulfide directly corroborates a proposed mechanism for the migration of elemental sulfur through carbon.

Introduction

Reticulated vitreous carbon (RVC) is a high void-volume elemental carbon foam with conductive and mechanical properties that make it useful as a space-filling electrode,[1,2] including nonstirred-cell coulometry. We previously used RVC electrodes to facilitate dynamic control of the oxidation state of *Azotobacter vinelandii* nitrogenase FeMoco in anaerobic *N*-methylformamide solution during spectroelectrochemical experiments using sulfur K-edge or molybdenum L-edge X-ray absorption spectroscopy (XAS).[3,4]

However, in the course of similar sulfur K-edge spectroelectrochemical investigations of the $[Fe_2S_2(S_{cys})_4]$ active site of spinach Ferredoxin I, dissolved in buffered aqueous solution, XAS spectra of both the oxidized ($Fe^{2+}-Fe^{3+}$ mixed-valent) and reduced sites were found to contain spurious sulfur K-edge absorption features. These were traced to sulfur within the RVC electrode and were modeled as sulfoxide, sulfonate, and sulfate.[5]

A previous elemental analysis of RVC reported 1% nitrogen and 0.5% hydrogen, along with traces of Fe, Al, Cu, and Ag, but did not mention sulfur.[6] RVC itself is produced by pyrolysis of synthetic resins[1,2] and so the origin of the observed sulfur is uncertain. However, sulfur is present

* To whom correspondence should be addressed. Phone: 1-650-723-2479. Fax: 1-650-723-4817. E-mail: Frank@ssrl.slac.stanford.edu.
† Department of Chemistry, Stanford University.
‡ Stanford Synchrotron Radiation Laboratory, Stanford University.
§ Current address: Laboratoire de Chimie Inorganique, URA 420, CNRS, Université de Paris-Sud, 91405 Orsay, France.

(1) Wang, J. *Electrochim. Acta* **1981**, *26*, 1721−1726.
(2) Friedrich, J. M.; Ponce-de-León, C.; Reade, G. W.; Walsh, F. C. *J. Electroanal. Chem.* **2004**, *561*, 203-217.
(3) Hedman, B.; Frank, P.; Hodgson, K. O.; Feldman, B. J.; Gheller, S. F.; Schultz, F. A.; Newton, W. E. Sulfur K and molybdenum L-edge XAS of the nitrogenase iron−molybdenum cofactor under in-situ electrochemical control. In *X-ray Absorption Fine Structure*; Hasnain, S. S., Ed.; Ellis Horwood: Chichester, U.K., 1991; pp 168−170.
(4) Schultz, F. A.; Feldman, B. J.; Gheller, S. F.; Newton, W. E.; Hedman, B.; Frank, P.; Hodgson, K. O. In *Near-Edge X-ray Spectroelectrochemistry at Low Energies, Cell Performance, and Application to Models and the Nitrogenase Cofactor*; Schultz, F. A., Taniguchi, I., Eds.; The Electrochemical Society: Pennington, NJ, 1993; Vol. 93−11, pp 108−117.
(5) Anxolabéhère-Mallart, E.; Glaser, T.; Frank, P.; Aliverti, G.; Zanetti, J.; Hedman, B.; Hodgson, K. O.; Solomon, E. I. *J. Am. Chem. Soc.* **2001**, *123*, 5444−5452.
(6) Strohl, A. N.; Curran, D. J. *Anal. Chim. Acta* **1979**, *108*, 379−383.

10.1021/ic0610637 CCC: $33.50
Published on Web 11/04/2006

in pitch and coal, which are used to produce some carbon foams,[7,8] and sulfur has been detected in carbon blacks[9] and speciated in certain asphaltenes, oils, and coals using sulfur K-edge XAS.[10−14] The response of carbon electrodes is affected by sulfur doping[15,16] and sulfur can irreversibly react with the lithium inserted into pyrolytic carbon battery electrodes.[17] Sulfur-doped carbon aerogels showed enhanced platinum uptake, followed by improved catalytic activity.[18] The electrode response of RVC varies systematically across virtually the entire range of pH;[6] a process in which any endogenous sulfur may play a part. RVC foams have also been evaluated as a matrix for bioreactors,[19−21] in flow-through reactors for stripping coulometry of environmentally important metal pollutants,[22,23] and as a substrate for surface-modified carbon electrodes.[2] Stripping coulometry of copper produces localized crystallites in RVC electrodes,[2,24,25] which imply preferred sites of growth. For these reasons, speciation of sulfur in RVC is of interest.

Here, using elemental analysis and sulfur K-edge XAS, we report the results of a detailed assessment of sulfur in native RVC and in RVC following oxidative surface modification. The oxidation states and the functionalities of the sulfur in each form of RVC were assayed by direct curve-fitting of the sulfur K-edge spectrum of RVC using the XAS spectra of appropriate models. An equilibrium thermodynamic approach to sulfur-reactive sites in RVC is outlined that allows proportionate intercomparison of sulfur types among batches of RVC.

Materials and Methods

RVC, 80 pores per inch (ppi), was purchased from ERG Materials and Aerospace Corporation (Oakland, CA) as rectangular prismatic sheets with approximate dimensions of 26 × 13 × 0.5 cm. The experimental samples were cut from these larger sheets using an exacto knife. A second 80 ppi sample of RVC was obtained from the "Idea-Pack" laboratory sample kit, also obtained from ERG. Surface-oxidized RVC was prepared from the purchased bulk as described earlier,[5] following the method of Fujihira and Osa.[26] In general, a small rectangular prism of RVC, about 25 × 5 × 5 mm, was soaked in 0.2 M $KMnO_4$ in 2 M aqueous H_2SO_4 for 45 min, after which time spontaneous submergence in water of the treated RVC was observed. This behavior was taken to indicate the production of a water-wettable interior surface. The modified RVC was then washed in a stream of deionized water for about 3 h to clear soluble adsorbents. Elemental analysis for sulfur in RVC was carried out by Galbraith Laboratories, Knoxville, TN, and the results were reported as ±1 ppm.

Solid models, including thiamine hydrochloride, 2-(4-chlorophenyl)-1-methylethyl-2,4-dinitrobenzene sulfenate, trimethylsulfonium iodide, thionin perchlorate, methylene blue, 3,3′-diethylthiacyanine iodide, *N*,*N*′-thiobisphthalimide, triphenylmethanesulfenamide, 2,1,3-benzothiadiazole, 3-(thianaphthen-3-yl)-L-alanine hydrochloride, sulfanilamide, sodium methyl sulfate, 1,2:5,6-di-O-isopropylidene-D-mannitol cyclic sulfate, 1,3-propanediol cyclic sulfate, and inositol hexasulfate were used as obtained from Aldrich Chemicals. The sulfur K-edge spectra of these compounds were measured using the solids finely ground in boron nitride and lightly spread on sulfur-free Mylar tape. The compounds (±)-6-thioctic amide and *trans*-1,2-dithiane-4,5-diol were likewise measured, but as finely ground neat powders. Cysteine, methionine, cystine, and oxidized glutathione were measured as 50−100 mM solutions in 250 mM pH 7.1 Tris citrate buffer. Solutions of elemental sulfur (52 mM in sulfur), ethylenesulfite (0.1 M), and bis(tert-dodecyl)pentasulfide (15 mM = 75 mM total sulfur) were made in *p*-xylene. The sulfur solution was passed through a 0.2 μm nylon filter prior to measurement. Ethylene episulfide (Aldrich Chemicals) was filtered through a 0.2 μm nylon filter to remove a fine suspension, and the clear straw-colored liquid was measured as a 0.1 M solution in *p*-xylene. Dimethylsulfite (Aldrich Chemicals) was distilled from anhydrous Na_2CO_3 and a low-boiling fraction was rejected. The clear colorless constant-boiling distillate (bp = 122−123 °C, uncorrected) was measured as a 0.1 M solution in *p*-xylene. The compound 2-(2-analinovinyl)-3-methylthiazolium iodide was finely dusted on Mylar tape and measured on SSRL beam line 4-1, with 70% detuning at 2740 eV. The sulfur K-edge XAS spectra of methionine sulfoxide and methionine sulfone, of sulfate in aqueous solutions of various pH values, and of methanesulfonic acid were reported earlier.[27−30] The sulfur K-edge XAS spectra of thianthrene, benzothiophene, and dibenzothiophene were kindly provided by Prof. Graham George, Department of Geological Sciences, University of Saskatchewan, Canada.

Except as noted above, sulfur K-edge XAS spectra were measured on the 54-pole wiggler beam line 6-2 at the Stanford Synchrotron Radiation Laboratory, SLAC, Stanford University, using a 10.4 kG wiggler field. XAS data were collected under dedicated ring conditions of 3 GeV and 60−100 mA. The radiation was energy discriminated using a Si(111) double-crystal monochromator (fully tuned at 2740 eV). A Ni-coated mirror was used

(7) Klett, J. W. U.S. Patent 6,033,506, 2000.
(8) Klett, J. W.; McMillan, A. D.; Gallego, N. C.; Walls, C. A. *J. Mater. Sci.* **2004**, *39*, 3659−3676.
(9) Roy, S. C.; Harding, A. W.; Russell, A. E.; Thomas, K. M. *J. Electrochem. Soc.* **1997**, *144*, 2323−2328.
(10) George, G. N.; Gorbaty, M. L. *J. Am. Chem. Soc.* **1989**, *111*, 3182−3186.
(11) Waldo, G. S.; Carlson, R. M. K.; Moldowan, J. M.; Peters, K. E.; Penner-Hahn, J. E. *Geochim. Cosmochim. Acta* **1991**, *55*, 801−814.
(12) Taghiei, M. M.; Huggins, F. E.; Shah, N.; Huffman, G. P. *Energy Fuels* **1992**, *6*, 293−300.
(13) Kasrai, M.; Brown, J. R.; Bancroft, G. M.; Yin, Z.; Tan, K. H. *Intl. J. Coal Geol.* **1996**, *32*, 107−135.
(14) Sarret, G.; Connan, J.; Kasrai, M.; Bancroft, G. M.; Charrie-Duhaut, A.; Lemoine, S.; Adam, P.; Albrecht, P.; Eybert-Berard, L. *Geochim. Cosmochim. Acta* **1999**, *63*, 3767−3779.
(15) Wu, Y. P.; Fang, S.; Jiang, Y.; Holze, R. *J. Power Sources* **2002**, *108*, 245−249.
(16) Zheng, W.; Liu, Y. W.; Hu, X. G.; Zhang, C. F. *Electrochim. Acta* **2006**, *51*, 1330−1335.
(17) Larcher, D.; Mudalige, C.; Gharghouri, M.; Dahn, J. R. *Electrochim. Acta* **1999**, *44*, 4069−4072.
(18) Baker, W. S.; Long, J. W.; Stroud, R. M.; Rolison, D. R. *J. Non-Cryst. Solids* **2004**, *350*, 80−87.
(19) Wang, J.; Naser, N. *Anal. Chim. Acta* **1991**, *242*, 259−266.
(20) Kent, B. L.; Matharasan, R. *J. Biotechnol.* **1992**, *22*, 311−327.
(21) Khayyami, M.; Garcia, N. P.; Larsson, P. O.; Danielsson, B.; Johansson, G. *Electroanalysis* **1997**, *9*, 523−526.
(22) Wang, J.; Dewald, H. D. *J. Electrochem. Soc.* **1983**, *130*, 1814−1818.
(23) Walsh, F. C.; Pletcher, D.; Whyte, I.; Millington, J. P. *J. Chem. Technol. Biotechnol.* **1992**, *55*, 147−155.
(24) Reade, G. W.; Bond, P.; de Leon, C. P.; Walsh, F. C. *J. Chem. Technol. Biotechnol.* **2004**, *79*, 946−953.
(25) Reade, G. W.; Nahle, A. H.; Bond, P.; Friedrich, J. M.; Walsh, F. C. *J. Chem. Technol. Biotechnol.* **2004**, *79*, 935−945.
(26) Fujihira, M.; Osa, T. *Prog. Batteries Sol. Cells* **1974**, *2*, 244−248.
(27) Frank, P.; Hedman, B.; Carlson, R. M. K.; Tyson, T. A.; Roe, A. L.; Hodgson, K. O. *Biochemistry* **1987**, *26*, 4975−4979.
(28) Smith, T. A.; DeWitt, J. G.; Hedman, B.; Hodgson, K. O. *J. Am. Chem. Soc.* **1994**, *116*, 3836−3847.
(29) Frank, P.; Hedman, B.; Carlson, R. M. K.; Hodgson, K. O. *Inorg. Chem.* **1994**, *33*, 3794−3803.
(30) Frank, P.; Hedman, B.; Hodgson, K. O. *Inorg. Chem.* **1999**, *38*, 260−270.

for harmonic rejection. All the XAS spectra were measured as the emission from fluorescence excitation, which was monitored using a Stern−Heald−Lytle fluorescence detector. Sulfur K-edge XAS spectra were calibrated against the maximum of the first sulfur K-edge feature of sodium thiosulfate, assigned to 2472.02 eV. Sodium thiosulfate calibration spectra were obtained periodically during data collection. The sulfur K-edge XAS spectra were averaged and normalized as described.[5,30] The sulfur K-edge spectra of RVC were fit using the PC version of the program DATFIT, which is part of the EXAFSPAK program suite written by Prof. Graham George, University of Saskatchewan. This analysis package is available free of charge at http://www-ssrl.slac.stanford.edu/exafspak.html. The DATFIT algorithm minimizes the residuals during a fit, producing the goodness of fit *F*-value calculated as $F = \sum(I_{obsd} - I_{calcd})^2/N$, where I_{obsd} and I_{calcd} are the observed and calculated normalized intensity, respectively, and N = number of points. The errors in the percents of fit components are given as estimated standard deviations (esd's), which are obtained from the diagonal elements of the variance−covariance matrix.[31] A final fit most closely reproduced both the XAS spectrum and the first derivative of the XAS spectrum.

Results

Three samples of 80 pores-per-inch (ppi) RVC were analyzed for the presence of elemental sulfur. These were native unmodified RVC, surface-oxidized RVC cut from the same batch of sheet stock, and a second native RVC sample taken from a set of free laboratory samples provided by ERG. The latter provided an independent measure of sulfur ubiquity in RVC. The total sulfur in these RVC samples, by weight, was found to be 733, 882, and 985 ppm, respectively. The subsequent XAS experiments were performed on samples taken from the same sheet-stock that was subjected to elemental analysis.

Figure 1a shows the sulfur K-edge XAS spectra of native RVC and RVC following surface oxidation with $KMnO_4/H_2SO_4$ (see the Materials and Methods section for the oxidation conditions). In sulfur K-edge XAS spectra, the energy positions of the rising edge maxima of oxido-sulfur compounds systematically shift 1.7±0.1 eV to higher energy per unit increase in formal sulfur valence, with a range of about 13 eV between S_8 and SO_4^{2-}.[11,27,32−34] In Figure 1, the high signal-to-noise spectra show that the ∼0.1% sulfur in RVC is readily detectable by XAS. The intense peaks at 2474.3 and 2482.4 eV reveal the presence of low- and high-valent sulfur, respectively. Comparing the first derivatives of the spectra in Figure 1b with the linear grid of eV/(oxidation state) indicates resident sulfur valences of approximately S^0, S^{1+}, S^{2+}, S^{5+}, and S^{6+}. Further inspection of Figure 1 reveals that the distribution of reduced and oxidized sulfur within RVC has been modified by permanganate oxidation.

For the K-edge XAS spectra to usefully discriminate among sulfur environments, relatively modest structural

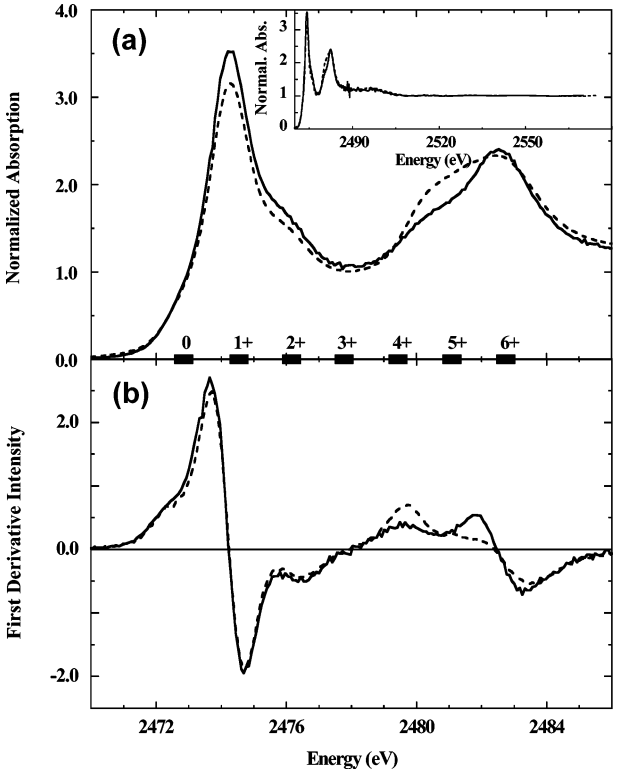

Figure 1. Sulfur K-edge XAS spectra (a) and first derivatives of the XAS spectra (b) of (—) native RVC and (- - -) $KMnO_4/H_2SO_4$-oxidized RVC. The abscissa is marked to show the energy regions where oxido-sulfur of serially increasing formal oxidation state may produce K-edge XAS absorption maxima. The inset shows the full energy-range sulfur K-edge XAS spectra showing that the two RVC spectra were equivalently normalized, which is a necessary condition for a comparative fit.

variations in sulfur-containing molecules must produce readily observable changes in sulfur K-edge spectra, even when the functional group of sulfur remains unchanged. Extensive literature already in existence demonstrates this sensitivity.[10,29,33−35] In Figure 2a−d (Supplemental Figure 1), we demonstrate this sensitivity by comparing the sulfur K-edge spectra of three different disulfides (panels a and b) and three different sulfate esters (panels c and d). These spectra were all measured using solid samples and thus exhibit the effect of self-absorption. However, this should not impact the validity of the comparisons based on the transition energies and multiplicities.

The structural formulas of the molecules in review are drawn in Scheme 1. Figure 2a and b shows the effect of differing disulfide geometries on sulfur K-edge XAS spectra. Variations in the energy positions of the two major transitions, between 2472 and 2475 eV reflect shifts of the empty C−S σ^* orbitals[36−39] induced by steric constraints upon bonding. Relative to cystine, strain within the five-membered

(31) Salter, C. *J. Chem. Educ.* **2000**, *77*, 1239−1243.
(32) Fahlman, A.; Hamrin, K.; Hedman, J.; Nordberg, R.; Nordling, C.; Siegbahn, K. *Nature (London)* **1966**, *210*, 4−8.
(33) Hedman, B.; Frank, P.; Penner-Hahn, J. E.; Roe, A. L.; Hodgson, K. O.; Carlson, R. M. K.; Brown, G.; Cerino, J.; Hettel, R.; Troxel, T.; Winick, H.; Yang, J. *Nucl. Instrum. Methods* **1986**, *A246*, 797−800.
(34) Pickering, I. J.; Prince, R. C.; Divers, T.; George, G. N. *FEBS Lett.* **1998**, *441*, 11−14.
(35) Pickering, I. J.; George, G. N.; Yu, E. Y.; Brune, D. C.; Tuschak, C.; Overmann, J.; Beatty, J. T.; Prince, R. C. *Biochemistry* **2001**, *40*, 8138−8145.
(36) Hitchcock, A. P.; Bodeur, S.; Tronc, M. *Phys. B* **1989**, *158*, 257−258.
(37) Foerch, R.; Urch, D. S. *J. Chem. Soc., Faraday Trans. 1* **1989**, *85*, 1139−1147.
(38) Dezarnaud, C.; Tronc, M.; Hitchcock, A. P. *Chem. Phys.* **1990**, *142*, 455−462.
(39) Chauvistré, R.; Hormes, J.; Hartmann, E.; Etzenbach, N.; Hosch, R.; Hahn, J. *Chem. Phys.* **1997**, *223*, 293−302.

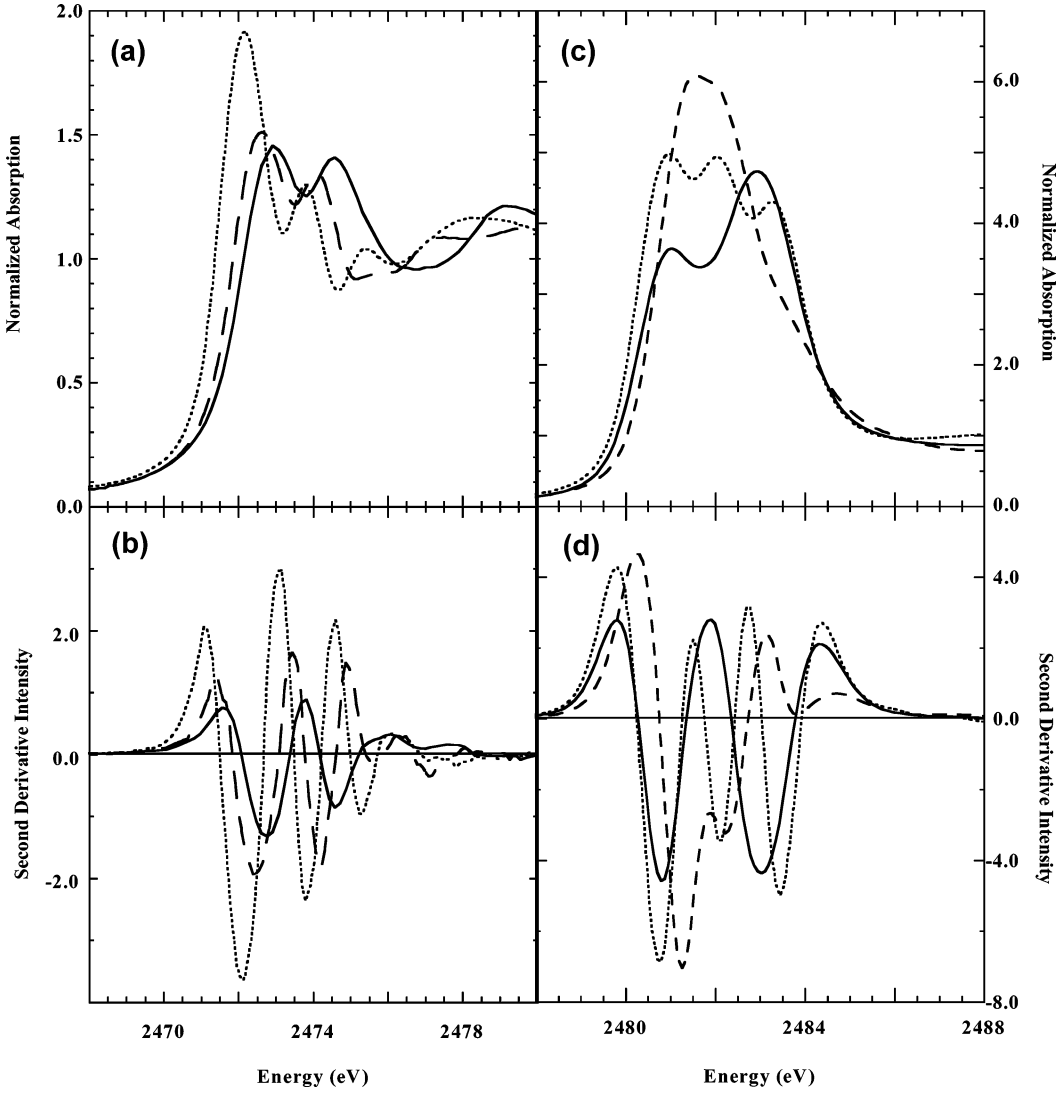

Figure 2. Sulfur K-edge spectra (top) and second derivatives of the XAS spectra (bottom) of (a and b) (—) cystine, (···) *trans*-1,2-dithiane-4,5-diol, and (- - -) (±)-6-thioctic amide (lipoamide disulfide) and (c and d) (—) D-*myo*-inositol hexasulfate, (- - -) 1,3-propylene cyclic sulfate, and (···) 1,2:5,6-di-*o*-isoprpylidene-D-mannitol cyclic sulfate. See Scheme 1 for the structural formulas.

ring of thioctic amide clearly affects the alkyl disulfide σ-bond orbital energies more than is the case within the 1,2-dithiacyclohexane, which is relatively strain free.[40,41]

Figure 2c and d compares the sulfur K-edge spectra of a set of carbon-sulfate esters. The molecular orbitals of free sulfate have been extensively explored using calculational models with varying degrees of sophistication.[42−50] These calculational models were recently extended using density functional theory (DFT), showing that the main white-line features result from electronic core-state transitions to the $6t_2$ and $7t_2$ virtual orbitals.[51] These consist primarily of sulfur 4p orbitals, and the antibonding sulfur 3p plus oxygen 2p orbitals, respectively. However, reorganization of the filled orbitals of sulfate upon bonding to carbon,[52] should be accompanied by changes in the mixing ratios and energy levels of the antibonding and virtual orbitals,[42] as happens when sulfate is complexed by metal ions.[51] This effect is evident in the spectrum of inositol hexasulfate, Figure 2c. The single observable transition at 2482.5 eV, typifying the free aqueous sulfate dianion,[53] has become two transitions split by 2.2 eV. The XAS spectroscopic differences are, if

(40) Burns, J. A.; Whitesides, G. M. *J. Am. Chem. Soc.* **1990**, *112*, 6296−6303.
(41) Bachrach, S. M.; Woody, J. T.; Mulhearn, D. C. *J. Org. Chem.* **2002**, *67*, 8983−8990.
(42) Cruickshank, D. W. J. *J. Chem. Soc.* **1961**, 5486−5504.
(43) Bishop, D. M.; Randic, M.; Morton, J. R. *J. Chem. Phys.* **1966**, *45*, 1880−1885.
(44) Bishop, D. M. *Theor. Chim. Acta* **1967**, *8*, 285−291.
(45) Hillier, I. H.; Saunders, V. R. *Chem. Commun.* **1969**, 1181−1182.
(46) Connor, J. A.; Hillier, I. H.; Saunders, V. R.; Barber, M. *Mol. Phys.* **1972**, *23*, 81−90.
(47) Szargan, R.; Koehler, H. J.; Meisel, A. *Spectrochim. Acta B* **1972**, *27*, 43−45.
(48) Johansen, H. *Theor. Chim. Acta (Berlin)* **1974**, *32*, 273−278.
(49) Piroumian, G. P.; Grigorian, G. G.; Beylerian, N. M. *Polyhedron* **1983**, *2*, 953−954.
(50) Sliznev, V. V.; Solomonik, V. G. *Russ. J. Coord. Chem.* **1996**, *22*, 655−660.
(51) Szilagyi, R. K.; Frank, P.; DeBeer, G. S.; Hedman, B.; Hodgson, K. O. *Inorg. Chem.* **2004**, *43*, 8318−8329.
(52) Whitfield, D. M.; Tang, T. H. *J. Am. Chem. Soc.* **1993**, *115*, 9648−9654.
(53) Frank, P.; Hodgson, K. O. *Inorg. Chem.* **2000**, *39*, 6018−6027.

Scheme 1

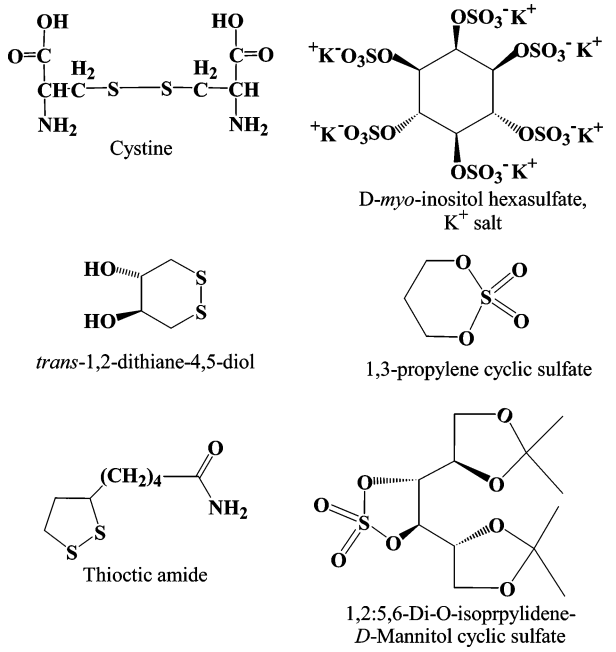

anything, more extreme for the two cyclic sulfate esters (Figure 2c and d). While the pentacyclic mannitol sulfate exhibits three partly resolved sulfur K-edge features, the XAS spectrum of the hexacyclic propylene sulfate consists of only a single broadened feature at 2481.6 eV. Examination of the second derivative XAS spectra (Figure 2d) reveals that propylene cyclic sulfate, like the mannitol derivative, also produces three sulfur K-edge XAS features, but at different energies (i.e., 2480.8, 2482.1, and 2483.4 eV for the mannitol cyclic sulfate and 2481.3, 2482.3, and 2483.8 eV for the propylene cyclic sulfate) and with different intensities. It is interesting to note that the change from a six- to five-membered ring in the cyclic sulfates is similar to that observable for the cyclic disulfides (Figure 2). That is, the structural change was accompanied by a shift of the XAS transitions to lower energy and an increase in the intensity of the highest-energy transition. These XAS spectral differences show that changes in the local structure of otherwise similar functional groups significantly re-order the orbital mixing and thus modify the energy positions and intensities of XAS spectral transitions. It is possible, therefore, to use K-edge spectra to distinguish among relatively minor structural variations of otherwise identical functional groups.

The second derivative of the sulfur K-edge XAS spectrum of the mannitol cyclic sulfate, Figure 2d, shows three relatively intense features at 2480.0, 2482.0, and 2483.3 eV that could readily be mistaken for a mixture of sulfur of valences 4+ (sulfone), 5+ (sulfonate), and 6+ (sulfate). A similar possibility derives from the two intense features of the inositol hexasulfate, which could be mistakenly assigned to a mixture of sulfur 5+ and 6+. These relatively intense multiple features indicate the necessity of directly modeling the sulfur K-edge XAS spectrum of an unknown with the XAS spectra of candidate sulfur compounds. This avoids errors in the assignment of sulfur functional groups that can

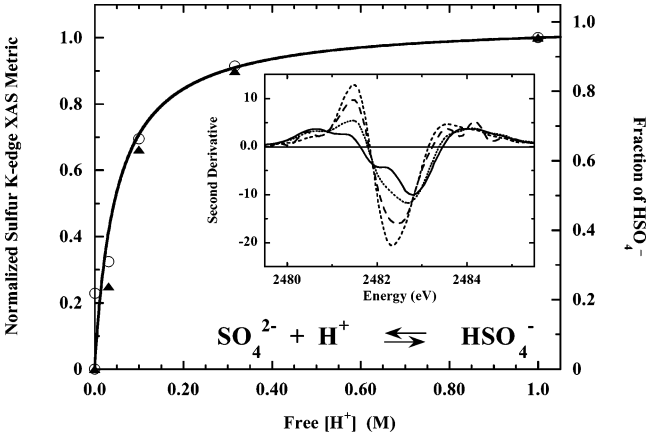

Figure 3. (○) fwhm and (▲) second derivative intensity of the 2482.4 eV feature of the K-edge XAS of sulfate ion in aqueous solution at varying pH values, plotted as normalized percent. The solid line is the titration curve of the HSO_4^- ion calculated using the known pK_a value of 1.92. The inset shows the second derivatives of the sulfur K-edge XAS spectra of sulfate ion at pH (—) 0.0, (···) 1.0, (– –), 1.5, and (- - -) 6.3 aqueous solution.

arise from descriptively correlating absorption features with oxidation state.

The data in Figure 3 show that sulfur K-edge XAS spectra of aqueous sulfate ion accurately reflect solution pH.[29,30] Acid−base equilibria also modify the respective K-edge XAS spectra of solution cysteine and of the aqueous Pb^{2+}, V^{3+}, and Ga^{3+} ions.[34,53−56] The complexation equilibria between chloride and actinides[57] and between the sulfate ion and $[V(H_2O)_6]^{3+}$ also affect the respective XAS K-edge spectra, including that of sulfate.[29,53] All these results together demonstrate that K-edge XAS spectra are observably modified by relatively subtle molecular perturbations and can usefully follow equilibrium reactivity.

In the consideration of the reliability of the small percentages for high-valent sulfur, the normalized XAS K-edge absorption maxima of oxidized sulfur are so intense that even a minor presence of these compounds produce significant K-edge XAS features. For example, the normalized intensities of the rising sulfur K-edge XAS maxima of solution-state sulfur, methionine sulfoxide, methionine sulfone, and sulfate ion are 4.4, 5.3, 7.8, and 10.8 normalized units, respectively. Thus even 2% sulfoxide or 1% sulfate will produce a rising edge feature with ∼0.1 normalized unit of intensity; a signal readily observable in sulfur K-edge spectra. For low-valent sulfur, the same criterion indicates that as little as 2−3% should be discernible to a K-edge fit.

Sulfur within vitreous carbon may conceivably include elemental grains, as well as covalent pseudo-aromatic or aliphatic-like sulfur, respectively, within graphitic or amorphous regions.[58] Endogenous acidic sulfur oxides, alterna-

(54) Strawn, D. G.; Sparks, D. L. *J. Colloid Interface Sci.* **1999**, *216*, 257−269.
(55) Frank, P.; Carlson, R. M. K.; Carlson, E. J.; Hodgson, K. O. *Coord. Chem. Rev.* **2003**, *237*, 31−39.
(56) Pokrovsky, O. S.; Pokrovski, G. S.; Schott, J. *J. Colloid Interface Sci.* **2004**, *279*, 314−325.
(57) Allen, P. G.; Bucher, J. J.; Shuh, D. K.; Edelstein, N. M.; Reich, T. *Inorg. Chem.* **1997**, *36*, 4676−4683.
(58) Bandosz, T. J.; Biggs, M. J.; Gubbins, K. E.; Hattori, Y.; Iiyama, T.; Kaneko, K.; Pikunic, J.; Thomson, K. T. *Chem. Phys. Carbon* **2003**, *28*, 41−228.

tively, must be pendant on carbon surfaces.[26,59,60] Elemental sulfur, pyrite, sulfide, thiophene, and sulfate have been detected in a variety of coals and asphaltenes.[10,11,14,61−65] However, the production of vitreous carbon foams involves high-temperature reductive pyrolysis of synthetic resins,[1,2,66,67] which do not include intentional sulfur. The origin of the observed sulfur in RVC is therefore somewhat obscure. However, the pyrolysis conditions must certainly modify the native distribution of any endogenous sulfur in the starting resins.[68−70]

In RVC, sulfur that has migrated into unusual or extended carbon environments may not produce an XAS spectrum that can be modeled by the XAS of any explicit small molecule. That is, although sulfur functional groups produce XAS K-edge spectra with characteristic rising edge energies, the electronic structure of a given molecular environment can modify the Z_{eff} of sulfur and thus shift a rising XAS K-edge by $\sim\pm0.3$ eV (Figure 2). Smaller energy shifts, up to $\sim\pm0.2$ eV, can be induced by variations in the physical environment, such as solution versus solid or protic versus nonpolar solvents. Further, long-range rigid molecular structures can produce unique sulfur K-edge XAS multiple scattering or continuum absorption features that cannot be produced by small molecules. Thus, a precise reproduction of the XAS spectrum of sulfur in RVC will not be entirely possible by means of curve-fitting using the XAS spectra of discrete sulfur-containing model compounds.

Nevertheless, the energy position and line-shape of a rising sulfur K-edge imposes strong constraints both on the choice of a specific functional group and on the choice of a molecular environment when fit-modeling a sulfur K-edge XAS spectrum. In addition, unique continuum transitions and multiple scattering features resulting from the local pseudo-molecular structure in RVC can further constrain the choice of small-molecule models.

With this in mind, therefore, we chose a variety of sulfur models ranging from S_8 to an array of organic environments consistent with graphitic, amorphous, and heterocyclic sites, including variations on thianthrene, thiophene, thiazole, aliphatic thiol and thioether, nitrogenous sulfur, and stepwise

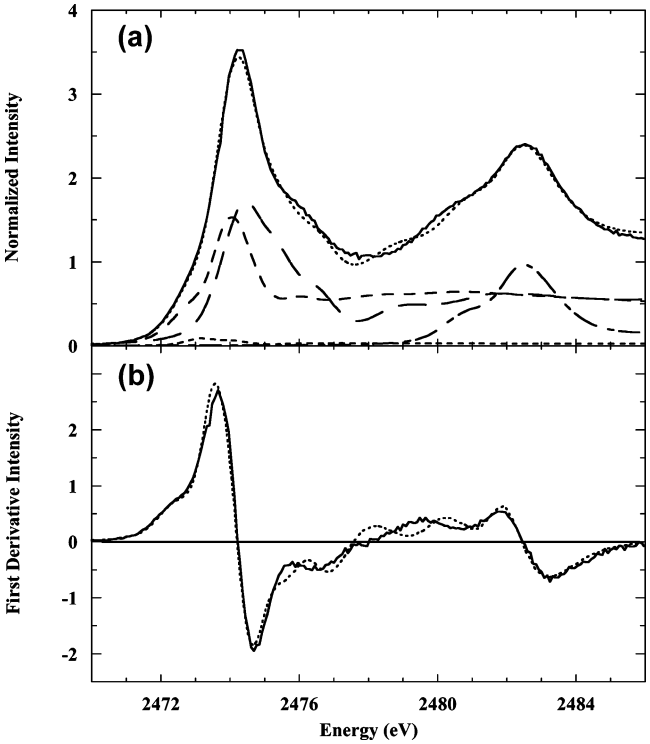

Figure 4. (a) Sulfur K-edge XAS spectrum of native RVC (—), the fit to the spectrum (···), and the components of the fit. To simplify presentation, the components have been combined as follows: (- - -) ethylene episulfide, (— —) neutral sulfur (as glutathione + thianthrene + benzothiophene), (— —) low-valent sulfur (as sulfenate ester + *N*,*N*′-thiobisphthalimide), and (— - —) oxidized sulfur (as methane sulfonic acid + inositol hexasulfate + sulfate dianion). (b) First derivatives of the sulfur K-edge spectrum of (—) native RVC and (···) the fit.

increases in sulfur oxidation state. With this array of models, fits to the sulfur K-edge XAS of RVC were obtained that appear to represent the functional groups and oxidation states of resident sulfur, as indicated by the good agreement between the energy positions of the features in the resulting fit spectrum and those of the RVC XAS data, and by the preferences manifested by the fit between similar but distinguishable forms of sulfur, as exemplified by Figure 2 and Scheme 1. Here we note in caution that unless K-edge XAS spectra are normalized consistently (Figure 1a, inset), fits can deviate from sample to sample in terms of the components preferred by the fit, producing incommensurate results.

Figure 4a and b shows the sulfur K-edge XAS spectrum of native RVC, along with the best fit to the spectrum. Among the neutral forms of sulfur tested and rejected by the fit were elemental sulfur, dialkyl pentasulfane, aliphatic thiol and thioether, thioketone, and thiourea. The presence of amorphous elemental sulfur[71−74] was not tested. However, amorphous sulfur is generally produced by quenching from

(59) Weinberg, N. L.; Reddy, T. B. *J. Appl. Electrochem.* **1973**, *3*, 73−75.
(60) Polania, A.; Papirer, E.; Donnet, J. B.; Dagois, G. *Carbon* **1993**, *31*, 473−479.
(61) Waldo, J. S.; Mullins, O. C.; Penner-Hahn, J. E.; Cramer, S. P. *Fuel* **1992**, *71*, 53−57.
(62) Huffman, G. P.; Shah, N.; Huggins, F. E.; Stock, L. M.; Chatterjee, K.; Kilbane, J. J., II; Chou, M.-I. M.; Buchanan, D. H. *Fuel* **1995**, *74*, 549−555.
(63) Wasserman, S. R.; Winans, R. E.; McBeth, R. *Energy Fuels* **1996**, *10*, 392−400.
(64) Gotte, V.; Rogalev, A.; Goulon, J.; Goulon-Ginet, C.; Michon, L.; Guilard, R.; Martin, D. *J. Phys. IV* **1997**, *7*, 667−668.
(65) Sarret, G.; Connan, J.; Kasrai, M.; Eybert-Berard, L.; Bancroft, G. M. *J. Synchrotron Radiat.* **1999**, *6*, 670−672.
(66) Noda, T.; Inagaki, M.; Yamada, S. *J. Non-Cryst. Solids* **1969**, *1*, 285−302.
(67) Gallego, N. C.; Klett, J. W. *Carbon* **2003**, *41*, 1461−1466.
(68) Calkins, W. H. *Energy Fuels* **1987**, *1*, 59−64.
(69) Sugawara, K.; Enda, Y.; Sugawara, T.; Shirai, M. *J. Synchrotron Rad.* **2001**, *8*, 955−957.
(70) Mullens, S.; Yperman, J.; Reggers, G.; Carleer, R.; Buchanan, A. C.; Britt, P. F.; Rutkowski, P.; Gryglewicz, G. *J. Anal. Appl. Pyrolysis* **2003**, *70*, 469−491.
(71) Tompson, C. W.; Gingrich, N. S. *J. Chem. Phys.* **1959**, *31*, 1598−1604.
(72) Winter, R.; Egelstaff, P. A.; Pilgrim, W. C.; Howells, W. S. *J. Phys. Cond. Matter* **1990**, *2* (Suppl. A), SA215-SA218.
(73) Winter, R.; Pilgrim, W. C.; Egelstaff, P. A.; Chieux, P.; Anlauf, S.; Hensel, F. *Europhys. Lett.* **1990**, *11*, 225−228.
(74) Eichinger, B. E.; Wimmer, E.; Pretorius, J. *Macromol. Symp.* **2001**, *171*, 45−56.

Table 1. Fit Components Normalized to 100%

modeling component	native RVC[a] (ratio)	oxidized RVC[a] (ratio)
ethylene episulfide	2.3 ± 2.0	4.3 ± 1.5
thianthrene	9.1 ± 2.1 (1)	6.8 ± 1.6 (1)
glutathione	10.1 ± 1.8 (1)	9.1 ± 1.3 (1)
sulfenate ester	11.9 ± 1.2 (1)	8.7 ± 0.9 (1)
benzothiophene	23.7 ± 1.8 (3)	22.0 ± 1.3 (3)
thiobisphthalimide	30.1 ± 1.2 (3)	29.9 ± 0.9 (4)
methionine sulfone	0.0	1.5 ± 0.2
methanesulfonic acid	1.2 ± 0.3	0.0
propylene cyclic sulfate	0.0	4.6 ± 0.4
inositol hexasulfate	6.0 ± 0.8	12.1 ± 0.7
sulfate	5.7 ± 0.6	1.0 ± 0.3

[a] The uncertainties are the estimated standard deviations numerically calculated by the fit.

the liquid state[75] and so was considered an unlikely inclusion. Dibenzothiophene was always eliminated in favor of benzothiophene (Supporting Information Figure 1), and cysteine and methionine models were invariably zeroed out in favor of thianthrene. Also rejected by the fit were partially cationic pseudo-aromatic sulfur, as in thiamine, thiacyanine, and methylene blue, and fully cationic sulfur, such as trimethylsulfonium. Among the excluded higher-oxidation states of sulfur were aliphatic sulfoxide, sulfinic acid, and sulfone, along with dimethylsulfite and ethylenesulfite, benzenesulfonamide, bisulfate, and propylenesulfate cyclic diester. Thiosulfate was also tested in several fits and was invariably excluded. As will be shown below, the sulfur excluded from oxidized RVC differed only in detail from this list.

In Figure 4a, the fit representing native RVC adequately reproduced the XAS spectral shapes in the low- and high-valent sulfur energy regions, around 2474 and 2482 eV, respectively. The poorer quality fit between 2475 and 2481 eV is discussed below. Total sulfur was dominated by aromatic sulfur (S^0) and nitrogenous sulfur (S^{2+}), along with a significant fraction of S^{1+} modeled as a sulfenic ester. Oxidized sulfur was dominated by a combination of free sulfate and sulfate monoester. Table 1 shows the list of specific components of the final fit. To simplify the presentation in Figure 4a, the components were combined into episulfide, neutral sulfur, low-valent sulfur [$S^{(1-2)+}$], and highly oxidized sulfur [$S^{(3-6)+}$]. Nearly 90% of the resident sulfur was found to be neutral to low valent, despite the intensity of the high-valent sulfur XAS features.

For neutral sulfur, a disulfide component, modeled as glutathione (E_{max} = 2472.6, 2474.2 eV), fit the immediate rising edge intensity at 2473 eV. Other disulfide XAS models, including cystine, thioctic acid, or *trans*-1,2-dithiane-4,5-diol did not produce an equivalent fit. Elemental sulfur, thionin perchlorate, and its structural conger methylene blue all have sulfur K-edge XAS maxima near 2472.4 eV, but these XAS models were likewise rejected by the fit algorithm. That is, a lower *F* value resulted when the contribution of these models was reduced to zero during the fit. Attempts to discern possible elemental sulfur grains, modeled as the self-absorption-broadened sulfur K-edge XAS of finely ground solid elemental sulfur,[35] were also unsuccessful. Elemental sulfur was also excluded even when the elemental sulfur K-edge XAS was allowed to float in energy position.

However, a full fit to the rising edge energy region of the sulfur K-edge XAS of RVC was not possible without inclusion of an ethylene episulfide XAS model. Excluding this component left an unfit region around 2472.5 eV that was especially obvious in the first derivatives of the XAS spectrum and the fit (Supporting Information Figure 2). Application of an energy offset of 0.35 eV to the XAS spectrum of ethylene episulfide was required to achieve the best fit. This offset is about twice the limits of XAS spectral reproducibility, but it is consistent with the energy shift associated with structural variations within a given sulfur functional group, as discussed above. Equivalently good fits could not be obtained with other candidate sulfur models that exhibited sulfur K-edge XAS maxima at about the same energy as ethylene episulfide (E_{max} = 2472.8 eV), even when the energy positions were allowed to float during the fit.

A comparison of the sulfur K-edge XAS spectra of ethylene episulfide, bis(tert-dodecyl)pentasulfide, and elemental sulfur (Supprting Information Figure 3), all of which include nearly or fully zerovalent sulfur, shows that the latter two compounds produce significant rising K-edge XAS intensities at lower energies than does ethylene episulfide, and they exhibit discrete transitions at significantly different energies. Likewise, the sulfur K-edge spectrum of thioketone (as thiocamphor) exhibited a sharp and intense feature at 2470.2 eV, fully 2.5 eV lower in energy than the rising edge of sulfur in RVC. These XAS spectroscopic discriminations demonstrate the physical basis for the bias toward the episulfide model exhibited by the fit. A 1,2-dithietane candidate can be excluded as the source for the 2472.5 eV XAS feature because of the extreme instability of this group.[41,76−78]

In Figure 4b, the first derivative of the fit reproduces the major low- and high-valent sulfur features, at 2474 and 2482 eV, respectively. The sulfur K-edge XAS spectrum of RVC itself is relatively featureless between 2476 and 2480 eV, where oxido-sulfur groups of formal valence 2+ to 4+ produce intense XAS K-edge absorption features.[10,11,27] These relatively intense rising edge maxima would ensure the appearance of features in this energy region of the RVC sulfur XAS spectrum if there were a significant presence (>10%) of intermediate oxidation state sulfur.

In the 2476−2481 eV range, the fit braids through the data, with minima near 2478 and 2480 eV. Most of the extra features in the fit are from continuum resonances in the XAS spectrum of the *N*,*N*′-thiobisphthalimide model (at 2476.3, 2478.3, and 2480.9 eV; see Supporting Information Figure 4). Continuum resonances in K-edge XAS spectra are transitions to p-symmetry virtual states that exist above the ionization threshold at energies uniquely determined by the

(75) Steudel, R.; Eckert, B. *Top. Curr. Chem.* **2003**, *230*, 1−79.

(76) Nicolaou, K. C.; Hwang, C. K.; Duggan, M. E.; Carroll, P. J. *J. Am. Chem. Soc.* **1987**, *109*, 3801−3802.

(77) Nicolaou, K. C.; DeFrees, S. A.; Hwang, C. K.; Stylianides, N.; Carroll, P. J.; Snyder, J. P. *J. Am. Chem. Soc.* **1990**, *112*, 3029−3039.

(78) Steliou, K.; Salama, P.; Yu, X. *J. Am. Chem. Soc.* **1992**, *114*, 1456−1462.

electronic structure. The inappropriate continuum resonances contributed to the fit by *N*,*N*′-thiobisphthalimide indicate that this model does not reproduce the extended structure of the nitrogenous sulfur site in RVC. However, two other models of nitrogenous sulfur of similar sulfur valence (i.e., triphenylmethylsulfenamide and 2,1,3-benzothiadiazole) were rejected by the fit, again showing the sensitivity of XAS fits to specific functionality. Likewise, non-nitrogenous forms of sulfur having a similar valence (e.g., the sulfur within sulfenate ester, trimethylsulfonium, or methylene blue) were also excluded. Thus, the *N*,*N*′-thiobisimide functional group itself is most likely the correct model for one type of sulfur in RVC, as indicated by the distinct preference of the fit, even though the extended carbon environment is almost certainly incorrect.

Many attempts were made to improve the fit to the RVC sulfur K-edge XAS spectrum in the 2480 eV region by including the XAS spectra of sulfoxide (E_{max} = 2476.3 eV), sulfinic acid (E_{max} = 2477.3 eV), sulfite diester (E_{max} = 2477.5 eV), sulfone (E_{max} = 2479.9 eV), or sulfonic acid (E_{max} = 2481.2 eV), but these components were rejected by the fit. We therefore attempted to improve the fit to the 2480 eV shoulder by enforced inclusion of one percent sulfone sulfur, with the best-fit percents of the other components held constant. Although the resulting fit indeed more closely matched the data at 2480 eV, it was noticeably poorer at 2482 eV. The fit *F* value also increased from 0.310×10^{-2} to 0.373×10^{-2}, indicating a poorer overall fit. The fit to the shoulder at 2480 eV improved further when the sulfate ester component (features at 2480.7 and 2482.8 eV) was floated to accommodate the enforced 1% sulfone, while keeping the rest of the component percents constant. However, the fit around the maximum at 2482 eV was again poorer because the percent of sulfate ester was reduced to compensate for the enforced intensity of the sulfone component. The *F* value of this fit (0.342×10^{-2}) was again worse than that of the fit without the imposed 1% sulfone. Fixed stepwise additions of methionine sulfone always resulted in a poorer fit, even when the percents of all the remaining components were allowed to float. The fit improved when the energy position of methionine sulfone was allowed to float, but the resulting shift in the sulfone rising K-edge energy position was so large (0.8 eV) that it rendered the model physically meaningless. A similar test with the methionine sulfoxide XAS model, added as a floated component, also excluded this functional group.

In a further attempt to improve the fit to high-valent sulfur, the XAS spectrum of native RVC was fit over the range of 2479−2490 eV to exclude the inappropriate continuum resonances stemming from the *N*,*N*′-thiobisphthalimide model. A linear offset was used to approximate the edge-jump intensity of the low-valent sulfur. However, the fit to the high-valent sulfur features was not improved despite testing combinations of all available models between S^{3+} (cysteine sulfinic acid) and S^{6+} (sulfate and sulfate esters). Finally, the energy positions of the high-valent sulfur models were floated to simulate the shift in sulfur Z_{eff} that might be produced by ostensible and varied RVC microenvironments. Very good fits to the high-energy sulfur K-edge features of RVC were then found, but the rising K-edge XAS energy position of at least one component always shifted by 0.4−1.2 eV, while shifts of 0.1−0.3 eV were imposed on all the remaining components. The former range could indicate variations of 0.25−0.7 formal valence units (see Figure 1) in sulfur Z_{eff} for a given functional group within RVC, which seems to be too great to reflect microenvironmental effects. In an alternative approach, fits using up to three instances of the same functional group were tested for environmentally induced shifts in Z_{eff}. These models were allowed to float in energy position to determine if they would distribute themselves over a small range in eV during the fit, thus modeling the effect of multiple environments. However the eV-shifts were again large and physically unreasonable.

Because of the failure of the above attempts to improve the fit, the central question resulting from the inaccuracies introduced by the *N*,*N*-thiobisphthalimide model into the fit is then whether the extraneous continuum resonances in the 2476−2481 eV energy region displaced low-level components from the fit that would otherwise have modeled a minority fraction of midvalent sulfur. Thus, an attempt was made to estimate the maximal percent of midvalent sulfur that could have remained unmodeled. The following analysis thus assumes that the negative unfit residuals represent the missing intensities of incorrectly excluded sulfur functional groups. The positive residuals are assumed to represent inappropriate intensities contributed by sulfur functional group models with incorrect extended molecular structures, which potentially excluded minor sulfur components that would otherwise have contributed to the fit. The unfit area was then quantified for each final fit as $\sqrt{[(\text{data minus fit})^2]}$. This method of calculation includes both the positive and negative unfit intensities and thus represents an upper limit of incorrectly excluded sulfur. For the native RVC fit over the full 2470−2486 eV range (Figure 4), the unfit area was 2.8% of the total normalized area of the sulfur K-edge XAS spectrum. For the truncated RVC XAS spectrum reflecting highly oxidized sulfur only, calculated over the range of 2479−2486 eV, the unfit residuals amounted to 2.0% of the normalized area. The analogous unfit percents for oxidized RVC (Figure 5; discussed below) were 2.3% and 1.6%, respectively. Therefore, only minor percents of intermediate valence sulfur might have been displaced from the fit by the inappropriate continuum resonances of inexact low-valent sulfur structural models.

For the sulfur K-edge spectrum of permanganate-oxidized RVC, a similar quality fit to the major sulfur features was obtained, shown in Figure 5a and b. The extra features imposed by the *N*,*N*′-thiobisphthalimide model again appear between 2476 and 2481 eV, especially in the first derivative of the fit. In the tested fits, many attempts were made to reproduce the broadened high-valent sulfur feature around 2481 eV in oxidized RVC. The same fitting strategy that was described above for native RVC was employed, including exploratory fits of the XAS data carried out over the limited range of 2478−2490 eV. However, inclusion of none of the additional high-valent sulfur models, as described

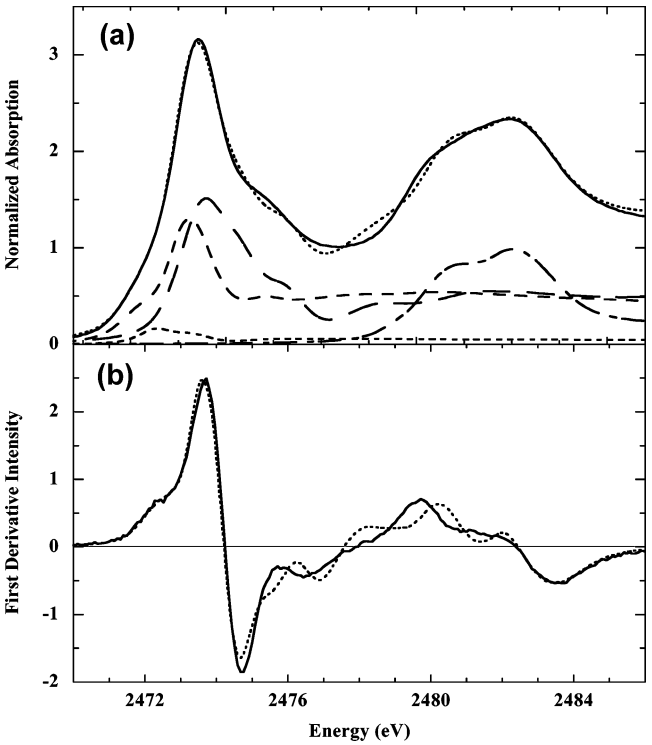

Figure 5. Sulfur K-edge XAS spectrum of (a) (—) oxidized RVC and (···) the fit to the spectrum. The components of the fit have been combined as (- - -) ethylene episulfide, (— —) neutral sulfur (as glutathione + thianthrene + benzothiophene), (— —) low-valent sulfur (as sulfenate ester + *N*,*N*′-thiobisphthalimide), and (— - —) oxidized sulfur (as methionine sulfone + 1,3-propanediol cyclic sulfate + inositol hexasulfate + sulfate). (b) First derivatives of the sulfur K-edge spectrum of (—) oxidized RVC and (···) the fit.

above in the fits to native RVC, improved the fit. Among several models, the set listed in Table 1 always gave the best fit.

Once again, the fit was dominated by low-valent sulfur, modeled by the same functional groups that fit the sulfur K-edge XAS spectrum of native RVC (Table 1). Low-valent sulfur thus proved strikingly resistant to oxidation. Only sulfenate sulfur showed a percentage decline greater than two standard deviations. Surprisingly, the alkyl sulfonate and the sulfate dianion found in native RVC were removed or diminished by the oxidation step. In contrast, the pendant sulfate monoester component represented by inositol hexasulfate more than doubled, and a small sulfone component could now be found. An entirely new component also appeared in the acceptance by the fit of 4.5% 1,3-propanediol cyclic sulfate. Every one of several attempts to include this component in the fit to native unoxidized RVC was rejected by the algorithm.

Additionally, the significant XAS spectroscopic changes that attend even modest structural variations about sulfur functional groups, as exemplified in Figures 2 and 3, and Supporting Information Figure 1, make unlikely the possibility that the major features in the sulfur K-edge XAS spectrum of RVC could be fit using sulfur functional group models that depart radically from the various forms of sulfur actually resident in RVC. Thus, the assignments of the functional groups episulfide, disulfide, sulfenate ester, *N*,*N*′-thiobisimide, sulfate, and sulfate ester are likely to be correct even if the extended molecular structures of the models are incorrect (as in *N*,*N*′-thiobisphthalimide).

Discussion

In the discussion of the sulfur K-edge XAS results, it is important to note at the outset that the 1/e penetration depth of 2.48 keV x-radiation into carbon is about 20 μm, while the pore-strut thickness of the 80 ppi RVC used in this study was about 100 μm.[2] Thus, the incident radiation sampled only about 20 vol % of the line-of-sight carbon. Within this moderate subsurface regime, the majority forms of sulfur found included S^0, $S^{\sim 0.5+}$, $S^{\sim 2+}$, and S^{6+} distributed among a variety of functional groups. No S^{3+} and only traces of S^{4+} and S^{5+} were detected.

The elemental analysis showed that the sulfur content in RVC (~0.1% w/w) can vary at least from batch to batch. The greater concentration of sulfur in the oxidized compared to the native RVC raises the possibility of sulfur infusion as a consequence of the oxidation process. The only source for additional sulfur might have been the 2 M sulfuric acid oxidation bath, and a potential mechanism for this process is described below. However the content of *free* sulfate dianion decreased following the oxidation, and the data in Table 1 show that the increase in *bound* sulfate can account for only about half of the excess sulfur found in oxidized RVC. This result implies that at least some of the excess sulfur detected in oxidized RVC was initially present in that sample. Likewise, the Idea Pack sample of native RVC included more sulfur than either the native RVC XAS sample or its oxidized homologue. If these results can be generalized, the sulfur content of RVC can apparently vary by ~±15% between production batches and by at least ~±4.5% within a single batch. This variation in absolute sulfur content will complicate an analysis comparing sulfur content following oxidative modification, and the discussion and derivation below specifically address this uncertainty.

If RVC were a truly amorphous glassy carbon, then it would be difficult to rationalize a reproducible and bounded set of sulfur sites. However, microscopic examination of RVC,[79] along with theoretical modeling,[80] indicate that glassy carbon has an ordered long-range structure. Vitreous carbon is known to be primarily sp^2 hybridized,[80−82] and electron microscopic studies have revealed tangles of collinear structures interpretable as ribbons of graphite-like sheets and Fullerene tubes, along with possible C_{60}-like Fullerene spheres.[80,83] Atomic-level reverse Monte Carlo simulations of vitreous carbon, using empirical electron-diffraction structure factors and pair-correlation data as target functions, predicted graphite-like sheets that are riddled with a variety of holes and variously sized rings ranging between three and nine carbons and that are buckled because of bond strain.[82]

(79) Dunne, L. J.; Clark, A. D.; Chaplin, M. F.; Katbamna, H. *Carbon* **1992**, *30*, 1227−1233.
(80) Harris, P. J. F. *Philos. Mag.* **2004**, *84*, 3159−3167.
(81) Robertson, J.; O'Reilly, E. P. *Phys. Rev. B* **1987**, *35*.
(82) O'Malley, B.; Snook, I.; McCulloch, D. *Phys. Rev. B* **1998**, *57*, 14148−14157.
(83) Townsend, S. J.; Lenosky, T. J.; Muller, D. A.; Nichols, C. S.; Elser, V. *Phys. Rev. Lett.* **1992**, *69*, 921−924.

The empirical regularities shown in Table 1 are additionally suggestive that the sulfur within separate samples of RVC inhabits a consistent set of pseudomolecular sites, compatible with a coherent reactivity. Taking all these results into account, we can derive a quantitative and systematic hypothesis explicating the reactivity and distribution of sulfur in RVC.

All of the RVC in a given batch should have experienced nearly identical conditions of thermal manufacture. If, during pyrolysis, the concentration of sulfur-reactive carbon defects in RVC was much larger than the concentration of migratory sulfur (i.e., $[C]_{reactive} \gg [S]_{total}$) and if a reactive equilibrium was attained, then within each production billet a minority species such as sulfur will have partitioned itself into an array of chemical states that will remain in approximate linear proportion no matter that the absolute sulfur concentration varies modestly about some mean across the billet. The full equilibrium−thermodynamic derivation of this model is given in the Supporting Information. In the context of equilibrium chemistry, quantitative comparisons across the sulfur functional groups can be made among various samples of RVC, including after chemical and physical treatment, despite small variations in the total sulfur concentration.

In support of the simplifying assumption that $[C]_{reactive} \gg [S]_{total}$, the gram-atomic ratio [C]/[S] for RVC is about 3300. The fit results correspondingly show a small and reproducible number of explicit sulfur functional groups, implicating a systematic set of sulfur-reactive sites in RVC carbon. Finally, the systematic defects in glassy carbon, as described above, are here suggested to be the latent precursors for the sulfur-reactive sites (see the derivation in the Supporting Information). All of these considerations taken together substantiate the thermodynamic model (cf. eq S1 and S2).

An analysis in terms of theory is strictly necessary because in the absence of an equilibrium thermodynamic model linking the partitioning of sulfur within glassy carbon to a common reaction theory, it would not be possible to compare the array of sulfur functionalities in any two RVC samples except in a phenomenological way. That is, in the absence of a conjoining theory, it would be impossible to relate the sulfur compositions of separate samples of RVC to a common causal framework. In that case, the fits to sulfur K-edge spectra would yield only a bare accounting of sulfur types, and no particular significance could be assigned to the appearance or disappearance of any sulfur functional groups following a physical or chemical treatment. Nor could any significance greater than coincidence be assigned to, for example, the discovery of a constant proportion among sulfur functional groups. Any discussion beyond an empirical tabulation would thus be pointless. Therefore, the theoretical model derived here is both central and critical to the following analysis. Most importantly, a testable predictive theory opens the way to a coherent understanding of the thermal reactions of sulfur or any other heteroelement in glassy carbon.

As required by the thermodynamic model, the ratios of nonpendant neutral and low-valent sulfur in native and surface-oxidized RVC are close to constant proportion (Table 1), within the limits imposed by the fit errors and the oxidative modification. The episulfide component was excluded from the ratioing because its uniquely high standard deviation, discussed below, rendered the percents too uncertain. To be fully successful, however, the equilibrium analysis also requires identifying the free sulfur, $[S]_{free}$, that is in equilibrium with the sulfur-reactive carbon sites.

Free sulfur in RVC, approximating migratory atomic sulfur, should be chemically distinct from bulk elemental S_8 and should produce a unique sulfur K-edge XAS spectrum. The absence of elemental sulfur from the fit is significant in this regard. Among all the modeled RVC sulfur functional groups, the discerned disulfide uniquely includes two sulfur atoms and a relatively weak sulfur−sulfur bond. This distinction points to the possibility that disulfide might be the source of mobile sulfur that, during pyrolysis, is in thermoreactive equilibrium with the defect sites in RVC that take up single sulfur atoms (eq S2).

The thermal reaction of these disulfide groups in RVC might involve extrusion of sulfur atoms, which then migrate to defect sites, as in eqs 1a and 1b

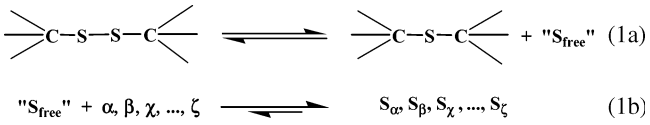

(1a)

(1b)

where α, β, χ, ..., ζ represent the carbon-reactive sites in RVC, and S_α, S_β, S_χ ..., S_ζ represent these sites following reaction with migratory sulfur, "S_{free}" (see the Supporting Information for details).

Disulfide sulfur would represent the source,[84,85] but not the identity, of $[S]_{free}$. The relative strengths of the C−S and S−S bonds[86] and reactions 1a and 1b predict that the proportion of disulfide should uniquely diminish with longer pyrolysis times, while the proportions of the other low-valent sulfur sites, except episulfide (see below), should increase. This prediction constitutes a strong test of the reaction 1 model. Reaction 1b should lie well to the side of products, and if reaction 1b were fast, then $[S]_{free}$ itself would always be small.[87] This idea could be tested using sulfur K-edge XAS spectra to determine the concentrations of the sulfur functional groups of a number of independent RVC samples that include $[S]_{total}$ varying across a modest range.

From the reaction scheme, it seems possible that the episulfide model might represent "S_{free}" in reaction 1 above and $[S]_{free}$ in the thermodynamic model (Supporting Information). Episulfides have been proposed as a diffusional species in the migration of atomic sulfur through carbon:[87,88] an idea that has both experimental and theoretical support.[89,90] In this scheme, the free sulfur, "S_{free}", of reaction 1 would migrate

(84) Wang, Z. Y.; Bonanno, G.; Hay, A. S. *J. Org. Chem.* **1992**, *57*, 2751−2753.
(85) Xu, L.; Yang, J.; Li, Y.; Liu, Z. *Fuel Proc. Technol.* **2004**, *85*, 1013−1024.
(86) Lide, D. R. Bond strengths in polyatomic molecules. In *Handbook of Chemistry and Physics* [Online], 85 ed.; Lide, D. R., Ed.; CRC Press: Boca Raton, FL, 2005. http://www.hbcpnetbase.com (accessed 2005).
(87) Humeres, E.; Peruch, M. d. G. B.; Moreira, R. F. P. M.; Schreiner, W. *Int. J. Mol. Sci.* **2005**, *6*, 130−142.
(88) Humeres, E.; Peruch, M. d. G. B.; Moreira, R. F. P. M.; Schreiner, W. *J. Phys. Org. Chem.* **2003**, *16*, 824−830.

across olefinic sites in RVC as transient episulfides. During pyrolytic manufacture, these episulfides would enter equilibrium with the more stable carbon-reactive sites available in RVC. The episulfides found in room temperature RVC would then reflect the equilibrium concentration trapped following cooling. However, the final concentrations of sulfur types in cold RVC may change from their hot equilibrium values during cooling, in that more facile equilibria may continue as hot RVC passes through progressively lower temperatures. Nevertheless, the results reported here represent the first direct detection of the episulfide intermediate proposed by others[87,88] to be the migratory form of sulfur within pyrolyzing carbon matrixes.

From Table 1, the percents of episulfide in native and oxidized RVC are statistically indistinguishable. Despite the large standard deviations marking the episulfide percents, in native RVC especially, the fact that the rising sulfur K-edge XAS of RVC could not be completely fit without inclusion of the episulfide model (discussion above and Supporting Information Figure 2) lends confidence that the result is real. Nevertheless, the fundamental chemical uncertainties described here point to the introductory nature of this study. For example, the rising edge intensity fit by the episulfide model may instead represent a microdispersed form of amorphous elemental sulfur structurally distinct from native S_8 and stabilized by the carbon matrix. The exclusion of bis-(^{t}dodecyl)-pentasulfide by the fits appears to obviate a linear sulfur catenate. However, sulfur trapped within carbon nanotubes[91] remains a candidate. Such sulfur is likely to be morphologically modified, in analogy to likewise trapped elemental selenium.[92] Clearly, testing the simple reaction model outlined above would require a much larger survey of sulfur within RVC.

In Table 1, there are five types of sites that fall under the purview of the above thermodynamic model, namely, those reflecting nonpendant neutral and low-valent sulfur. These groups are all consistent with stable forms of sulfur functional groups that might result from thermal reaction at carbon-defect sites under reducing conditions. All were resistant to oxidation despite a facile oxidative chemistry,[93,94] thus revealing them to be part of the subsurface RVC matrix. As required by the assumptions governing the above analysis, these sites are all in reasonably constant proportion within the two RVC samples, despite the difference in absolute sulfur concentrations. Thus, on this basis, it is possible to compare the proportionate changes of sulfur in the native and oxidized samples of RVC.

In general, thiol, thioether, and disulfide are among the sulfur functional groups most readily lost as H_2S during pyrolysis.[68] The fits indicate the former two functional groups are likely to be rare or absent in all native RVC. The considerable disulfide modeled by the fit is therefore surprising. However, disulfide, as opposed to −SH and $-SCH_3$ groups, need not be pendant on surfaces. Resistance of disulfide to oxidation by aqueous permanganate implies a subsurface locale, which might contribute to a kinetic stability. The new thioether group produced by the disulfide decomposition of reaction 1 might be any of the remaining low-valent sulfur models.

Among the forms of sulfur modeled in the fit perhaps the most surprising was the high proportion of nitrogenous sulfur, represented by *N*,*N*′-thiobisphthalimide. Nitrogen in carbon has been investigated using XPS and classified as either "graphenic" or "conjugated," the latter meaning "−C═N−".[15] However, neither of these categories describes the imido-nitrogen implied by *N*,*N*′-thiobisphthalimide. Further, rejection by the fit of the $(-C{=}N)_2S$ grouping, represented by 2,1,3-benzothiadiazole, appears to exclude "conjugated" nitrogen from the sulfur milieu. On the other hand, oxidized graphitic carbon is known to include an array of terminal carboxylate, ester, and anhydride groups.[59,60,95,96] It therefore seems reasonable to suppose that these groups represent the sites at which reduced nitrogen might react to produce phthalimide-like groups during pyrolytic manufacture. We did not analyze the RVC samples for elemental nitrogen; however thermal oxidation of carbons in O_2-N_2 mixtures produced surfaces containing ∼3 atomic % nitrogen.[97] The single published elemental analysis of RVC reported finding 1% nitrogen (see above), which represents a ∼20-fold greater atomic concentration than sulfur. Thus, the finding that 25−30% of the sulfur is apparently bound to nitrogen even in the overwhelming presence of carbon appears to indicate a strong thermodynamic gradient toward nitrogen−sulfur bonds. Whether this gradient is driven by the coexclusion of nitrogen and sulfur from the carbon network or by the N−S bonding interaction itself is unknown.

Benzothiophene and thianthrene sites in have been previously found in carbon.[10,11,61,68,69,98] Both molecules are known to be relatively stable under pyrolysis conditions.[99] The small amount of sulfone appearing in oxidized RVC nearly corresponds to the small decrease in the benzothiophene component, conversely indicating a small surface presence for this functional group. The small decrease in the *N*,*N*′-thiobisphthalimide model has not been traced to the sulfur K-edge XAS spectrum of the homologous oxidation product, a bisimidosulfamate, because of the present lack of an appropriate model. The greatest loss of reduced sulfur upon oxidation was found for sulfenic sulfur (Table 1).

Newly oxidized sulfur appeared almost exclusively as pendant sulfate monoester and cyclic sulfate diester. The

(89) Green, M.; Verkoczy, B.; Lown, E. M.; Strausz, O. P. *Can. J. Chem.* **1985**, *63*, 667−675.
(90) McKee, M. L. *J. Am. Chem. Soc.* **1986**, *108*, 5059−5064.
(91) Loiseau, A.; Pascard, H. *Chem. Phys. Lett.* **1996**, *256*, 246−252.
(92) Chancolon, J.; Archaimbault, F.; Bonnamy, S.; Traverse, A.; Olivi, L.; Vlaic, G. *J. Non-Cryst. Solids* **2006**, *352*, 99−108.
(93) Freeman, F.; Bond, D. L.; Chernow, S. M.; Davidson, P. A.; Karchefski, E. M. *Intl. J. Chem. Kinet.* **1978**, *10*, 911−922.
(94) Aitken, R. A.; Mesher, S. T. E.; Ross, F. C.; Ryan, B. M. *Synthesis* **1997**, 787−791.
(95) Yue, Z. R.; Jiang, W.; Wang, L.; Gardner, S. D.; Pittman, C. U. *Carbon* **1999**, *37*, 1785−1796.
(96) Ros, T. G.; van Dillen, A. J.; Geus, J. W.; Koningsberger, D. C. *Chem.—Eur. J.* **2002**, *8*, 1151−1162.
(97) Lee, W. H.; Lee, J. G.; Reucroft, P. J. *Appl. Surf. Sci.* **2001**, 136−142.
(98) Poleunis, C.; Vanden Eynde, X.; Grivei, E.; Smet, H.; Probst, N.; Bertrand, P. *Surf. Interface Anal.* **2000**, *30*, 420−424.
(99) Winkler, J. K.; Karow, W.; Rademacher, P. *J. Anal. Appl. Pyrolysis* **2002**, *62*, 123−141.

almost complete loss of the free sulfate ion itself is likely a result of the final washing of oxidized RVC. From Table 1, the net neutral and sulfenic sulfur lost during oxidation amounted to 8.4 ± 1.6%, while the increase in sulfate monoester plus sulfone was 7.6 ± 0.8%. These values are statistically indistinguishable. The 4.6% of newly appearing cyclic sulfate ester is thus not accountable by any corresponding loss of reduced sulfur. It is possible, therefore, that the cyclic sulfate ester originated from the exogenous sulfuric acid oxidation bath. At least two possible mechanisms for sulfate diester incorporation into RVC carbon can be envisioned. The first is direct acid-catalyzed sulfate addition across graphenic olefins, in analogy to small molecule chemistry.[100] However, the soaking in 8 M sulfuric acid did not produce sulfate groups in glassy carbon,[101] making the small-molecule analogy less likely. A second more intriguing possibility might be the electrophilic activation of sulfate in the form of the known permanganosulfate complex ion, $[O_3MnOSO_3]^-$, following condensation of H_2SO_4 with MnO_4^-.[102,103] Electrophilically activated sulfate might directly add across an olefin with a concomitant two-electron reduction of the electrophile. This proposal is supported by the analogous electrophilic reaction of phenyliodososulfate with olefins, directly producing cyclic sulfates plus iodobenzene.[104] Although permanganosulfate is known only in oleum solutions, this complex might form in the $KMnO_4$/H_2SO_4 oxidizing bath near the hydrophobic surfaces of RVC, where the activity of water is low.[105−107] Sulfuric acid has also been reported to form an ordered phase organized by the molecular orbitals at the surface of carbon nanotubes immersed in oleum.[108] If a similar phase formed near the hydrophobic surface of RVC in sulfuric acid solution, a more strongly acidic local milieu might be facilitated. In the reaction of the $[O_3MnOSO_3]^-$ ion with an RVC olefinic site, cyclic sulfate formation would be driven by the accompanying two-electron reduction of Mn(VII).

The surface pendant sulfur in RVC is most likely in the reduced state following pyrolytic manufacture,[68−70] which implies autoxidation to −SOR, $-SO_3^-$, $-OSO_3^-$, and SO_4^{2-} (R═H or alkyl) with the passage of time in air. In native RVC, the first and last members of the series dominate the population of oxidized sulfur. The totality of sulfur functional groups discerned to be in native and oxidized RVC are listed in Table 2. The total parts per million of each functional group and the standard deviations were calculated by combining the values in Table 1 with the total sulfur found by elemental analysis.

Table 2. Sulfur Functional Groups Found in Native and Oxidized RVC (ppm)

sulfur functional	RVC native	RVC oxidized	excluded sulfur
$(>C)_2(S)_{epi}$	17 ± 15	38 ± 13	S^0
−C−S−S−C−	74 ± 13	80 ± 11	$R-S_5-R$[f]
cyclo-5(═C−S−C═)[a]	174 ± 13	194 ± 11	−C−S−R (R is CH_3, H)
cyclo-6(═C−S−C═)[b]	67 ± 15	60 ± 11	>C═S[g]
−C−S−OR[c]	87 ± 9	77 ± 8	−C═N−S−N═C−[h]
$-(OC)_2N-S-N(CO)_2-$[d]	221 ± 9	264 ± 8	$-C-S^+<C_2-$[i]
$-C-S(=O)_2-C-$	0	13 ± 2	$>N^+=C-S-$[j]
$-C-SO_3-$	9 ± 2	0	$-C-S-NH_2$[k]
−C−O(O)S(O)O−C−[e]	0	41 ± 4	−C−S(═O)−C−
$-C-OSO_3^-$	44 ± 6	107 ± 6	−C−S(═O)OH
SO_4^{2-}	42 ± 4	9 ±3	−C−O−S(═O)−O−C−-C−SO_2NH_2[l]

[a] As benzothiophene. [b] As thianthrene. [c] As 2-(4-chlorophenyl)-1-methylethyl-2,4-dinitrobenzenesulfenate. [d] As thiobisphthalimide. [e] As 1,2:5,6-di-*o*-isopropylidene-D-mannitol cyclic sulfate. [f] As bis(tert-dodecyl)pentasulfide, linear sulfur catenate. [g] As thiourea. [h] As 2,1,3-benzothiadiazole. [i] As trimethylsulfonium. [j] As *N*-alkylthiazolium and *N*-alkyl-4,5-dihydrothiazolium. [k] As triphenylmethylsulfenamide. [l] As sulfanilamide.

As a final note, the electrodeposition of heavy metals onto unmodified RVC during flow-through processes has been investigated as a method of water remediation.[2,22,23] Electrode deposition of copper and other metals from solutions of the ions does not produce uniform films but rather isolated islands of surface crystallites.[2,22] The presence of pendant sulfate esters suggests that even native RVC should have ion-exchange properties.

The sulfate-dependent ion exchange capacity of native RVC can be assessed by the following estimate of surface coverage by sulfate groups. Porosity 80 ppi RVC has about 50 cm^2 of surface area/cm^3.[2,109] The volume of carbon per cubic centimeter of of RVC is then (density of RVC/density of glassy carbon[110]) 0.043 g cm^{-3}/1.48 g cm^{-3} = 0.029 cm^3 of carbon/cm^3 of 80 ppi RVC. The surface-to-volume ratio of carbon in one cubic centimeter of RVC is given by (carbon surface area/carbon volume) = 50 cm^2/0.029 cm^3 = 1724 cm^2 of carbon surface/cm^3 of RVC carbon. If all of the detected sulfate esters were confined to the surface of 80 ppi RVC, the upper limit of fractional coverage in native RVC would be, from Table 2, (ppm of sulfate in RVC carbon × carbon surface-to-volume ratio) ÷ (total surface area per cc of RVC) = ($44 \times 10^{-6} \times 1724$ cm^2 $cm^{-3} \div 50$ cm^2 cm^{-3}) × 100 = 0.15% of the native RVC surface would offer sulfate groups, assuming the cyclic sulfate esters readily hydrolyze to pendant monoesters. Correspondingly, for RVC oxidized with $KMnO_4/H_2SO_4$, about 0.51% of the surface would be occupied by sulfate ester groups. If a pendant sulfate group covered ∼3 Å^2 of carbon surface, then the percent coverage corresponds to about 0.4 μmol and 1.8 μmol of pendant sulfate monoesters/1000 cm^3 of RVC, respectively. A significant population of anionic sites on RVC

(100) Itokawa, H.; Matsumoto, H.; Nagamine, S.; Totsuka, N.; Watanabe, K. *Chem. Pharm. Bull.* **1988**, *36*, 3161−3163.
(101) Bowers, M. L.; Hefter, J.; Dugger, D. L.; Wilson, R. *Anal. Chim. Acta* **1991**, *248*, 127−142.
(102) Mishra, H. C.; Symons, M. C. R. *J. Chem. Soc. Abstr.* **1962**, 4411−4417.
(103) Gillespie, R. J.; Kapoor, R. *Can. J. Chem.* **1987**, *65*, 2665−2669.
(104) Robinson, R. I.; Woodward, S. *Tetrahedron Lett.* **2003**, *44*, 1655−1657.
(105) Bellisset-Funel, M.-C.; Sridi-Dorbez, R.; Bosio, L. *J. Chem. Phys.* **1996**, *104*, 10023−10029.
(106) Scatena, L. F.; Brown, M. G.; Richmond, G. L. *Science* **2001**, *292*, 908−912.
(107) Mowla, D.; Do, D. D.; Kaneko, K. *Chem. Phys. Carbon* **2003**, *28*, 229−262.
(108) Zhou, W.; Fischer, J. E.; Heiney, P. A.; Fan, H.; Davis, V. A.; Pasquali, M.; Smalley, R. E. *Phys. Rev B* **2005**, *72*, 045440/1−045440/5.
(109) ERG Materials and Space. http://www.ergaerospace.com/duocel/rvc.shtml.
(110) Van der Linden, W. E.; Dieker, J. W. *Anal. Chim. Acta* **1980**, *119*, 1−24.

surfaces could provide the loci where transition metal cations can bind and become reduced, seeding the scatter of crystallites that are observed on RVC surfaces following stripping electrolysis.

This study has shown that X-ray absorption spectroscopy can detail the structural status of sulfur in carbon foams and support a thermodynamic description of the thermal reactivity of sulfur in carbon. A similar assessment of other heteroatoms should also be possible, thus providing a detailed understanding of the chemistry of foreign elements in carbon materials.

Acknowledgment. This work was supported by Grant NIH RR-01209 (to K.O.H.). E.A.-M. gratefully acknowledges the CNRS and DOE BER for support during her stay at Stanford. XAS data were measured at SSRL, which is supported by the Department of Energy, Office of Basic Energy Sciences Division. The SSRL Structural Molecular Biology Program is supported by the National Institutes of Health, National Center for Research Resources, Biomedical Technology Program and by the Department of Energy, Office of Biological and Environmental Research (BER).

Note Added after ASAP Publication. This article was released ASAP on November 4, 2006, with an error in ref 4 and with a reference missing in the Supporting Information. The correct versions were posted on November 8, 2006.

Supporting Information Available: Figures showing the rising edge energy regions and the sulfur K-edge XAS spectra and a discussion of the derivation of the thermodynamic reaction model. This material is available free of charge via the Internet at http://pubs.acs.org.

IC0610637